



## Environmental controls on ecosystem-scale CH<sub>4</sub> emission from polygonal tundra in the Lena River Delta, Siberia

Torsten Sachs,<sup>1</sup> Christian Wille,<sup>2</sup> Julia Boike,<sup>1</sup> and Lars Kutzbach<sup>2</sup>

Received 1 June 2007; revised 13 December 2007; accepted 20 February 2008; published 15 July 2008.

[1] We present the first ecosystem-scale methane flux data from a northern Siberian tundra ecosystem covering the entire snow-free period from spring thaw until initial freeze-back. Eddy covariance measurements of methane emission were carried out from the beginning of June until the end of September in the southern central part of the Lena River Delta (72°22'N, 126°30'E). The study site is located in the zone of continuous permafrost and is characterized by Arctic continental climate with very low precipitation and a mean annual temperature of  $-14.7^{\circ}\text{C}$ . We found relatively low fluxes of on average  $18.7 \text{ mg m}^{-2} \text{ d}^{-1}$ , which we consider to be because of (1) extremely cold permafrost, (2) substrate limitation of the methanogenic archaea, and (3) a relatively high surface coverage of noninundated, moderately moist areas. Near-surface turbulence as measured by the eddy covariance system in 4 m above the ground surface was identified as the most important control on ecosystem-scale methane emission and explained about 60% of the variance in emissions, while soil temperature explained only 8%. In addition, atmospheric pressure was found to significantly improve an exponential model based on turbulence and soil temperature. Ebullition from waterlogged areas triggered by decreasing atmospheric pressure and near-surface turbulence is thought to be an important pathway that warrants more attention in future studies. The close coupling of methane fluxes and atmospheric parameters demonstrated here raises questions regarding the reliability of enclosure-based measurements, which inherently exclude these parameters.

**Citation:** Sachs, T., C. Wille, J. Boike, and L. Kutzbach (2008), Environmental controls on ecosystem-scale CH<sub>4</sub> emission from polygonal tundra in the Lena River Delta, Siberia, *J. Geophys. Res.*, 113, G00A03, doi:10.1029/2007JG000505.

### 1. Introduction

[2] Approximately 24% of the Northern Hemisphere's exposed land area is underlain by permafrost [Zhang *et al.*, 1999]. Permafrost-affected Arctic tundra has been a major carbon sink throughout the Holocene and is a globally significant carbon reservoir, although estimates of its size vary. For example, Post *et al.* [1982] estimate Arctic tundra environments to account for 190 Gt or 13–15% of the global soil organic carbon pool, while more recent studies suggest a carbon content of 500 Gt in frozen yedoma sediments alone. Yedoma is a Pleistocene-age loess permafrost with high volumetric ice content of 50–90% and 2–5% organic carbon [Zimov *et al.*, 2006a]. An additional carbon content of 400 Gt is estimated for nonyedoma permafrost excluding peatlands. This would exceed the carbon content of the atmosphere (730 Gt) and that of vegetation (650 Gt) [Zimov *et al.*, 2006a]. Because of the high sensitivity of high-latitude ecosystems to climate

changes, as well as their large proportion of the terrestrial earth surface, these landscapes are critically important for the Earth System, in particular for the global carbon cycle [Chapin *et al.*, 2000], as recent warming of the Arctic makes an increasing amount of previously frozen organic carbon available for decomposition.

[3] Where permafrost thaws, organic matter is decomposed by microbial activity. Yedoma soils contain very labile organic carbon, a large fraction of which is respired quickly upon thaw [Zimov *et al.*, 2006b]. Under aerobic conditions, this process produces carbon dioxide. Under anaerobic conditions, however, microbial decomposition produces methane.

[4] Northern wetlands and tundra are a major source of methane, contributing about 20% of the annual natural emissions [Fung *et al.*, 1991; Cao *et al.*, 1996; Christensen *et al.*, 1996]. With growing concern about climate change and the need to quantify emissions on a large scale, the greenhouse gas (GHG) budgets of arctic wetlands have come into the focus of attention. Because methane has a 23-fold global warming potential compared to carbon dioxide (time horizon of 100 years [Intergovernmental Panel on Climate Change, 2001]), even a modest change in methane sources can change the sign of the GHG budget of these landscapes [Friborg *et al.*, 2003; Corradi *et al.*, 2005] and feed back on the radiative forcing of the climate system.

<sup>1</sup>Research Unit Potsdam, Alfred Wegener Institute for Polar and Marine Research, Potsdam, Germany.

<sup>2</sup>Institute of Botany and Landscape Ecology, Ernst Moritz Arndt University of Greifswald, Greifswald, Germany.

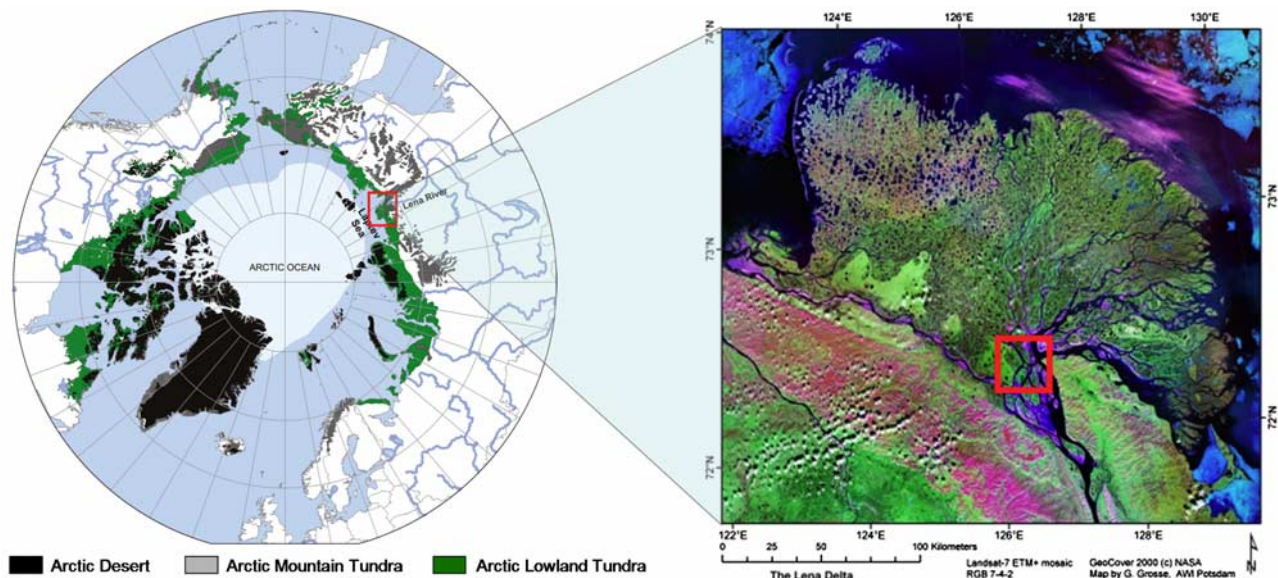


**Figure 1.** (left) Location of the investigation area and vegetation zones in the Arctic (modified after work by *UNEP/GRID-Arendal* [1996]). (right) Location of the study site Samoylov Island in the Lena River Delta (marked by the square (satellite image: Landsat 7 Enhanced Thematic Mapper (on Nimbus 6)+ GeoCover 2000, NASA (Landsat imagery courtesy of NASA Goddard Space Flight Center and U.S. Geological Survey))).

Furthermore, global climate models rely on predictions of future GHG concentrations, which require the ability to accurately model sinks and sources of methane as a powerful greenhouse gas.

[5] However, there is still much uncertainty about the source strength and the driving forces of methane flux of tundra landscapes. Existing studies of high-latitude methane fluxes were mostly based on the closed-chamber technique, which provides measurements representative on the very small scale. Because of the high temporal and spatial variability of methane fluxes [*Christensen et al.*, 1995, 2000; *Kutzbach et al.*, 2004, *Whalen and Reeburgh*, 1992], this technique alone does not give reliable information on landscape-scale fluxes. In addition, during chamber measurements the soil surface is isolated from the atmosphere so that the coupling of atmosphere and methane emission cannot be studied. The eddy covariance technique provides nonintrusive spatially integrated flux data at the landscape scale. However, to our knowledge only five studies reported eddy covariance methane flux data from Arctic tundra ecosystems, namely *Fan et al.* [1992] from western Alaska, *Harazono et al.* [2006] from northern Alaska, *Friberg et al.* [2000] from Greenland, and *Hargreaves et al.* [2001] from a semiarctic Finnish site. *Wille et al.* [2008] reported data from the Lena River Delta, Siberia, using measurements from 2 years to construct a “synthetic” growing season.

[6] Here, we present the first eddy covariance methane flux data covering an entire contiguous growing season in a Siberian Arctic tundra landscape. The objective of this study is (1) to quantify the methane emission over the full course of the growing season from snowmelt to freeze-back of the active layer, (2) to identify the biological and physical parameters which control the methane fluxes on the ecosystem scale, and (3) to test a model proposed by *Wille et al.*

[2008] for the same investigation site and validate it with a new and continuous data set. We found relatively low methane fluxes, which were predominantly controlled by atmospheric parameters (turbulence and pressure). A model based on turbulence, pressure, and soil temperature performed significantly better than a model without an atmospheric pressure term by *Wille et al.* [2008].

## 2. Site Description

[7] The study site is located on Samoylov Island, 120 km south of the Arctic Ocean in the southern central Lena River Delta (72°22'N, 126°30'E) (Figure 1). With an area of approximately 32,000 km<sup>2</sup> it is the largest delta in the Arctic and one of the largest in the world [*Walker*, 1998]. A maze of river channels and more than 1500 islands make up three main geomorphological terraces, only the youngest of which represents modern delta landscapes [*Are and Reimnitz*, 2000]. Samoylov Island (Figure 2) is considered representative of this Late Holocene terrace, which covers about 65% of the total delta area. Over the past ten years it has been the focus of a wide range of studies on surface-atmosphere gas and energy exchange, soil science, hydrobiology, microbiology, cryogenesis, and geomorphology [*Hubberten et al.*, 2006].

[8] The region is characterized by true arctic continental climate with very low temperatures and low precipitation. Mean annual air temperature at the meteorological station on Samoylov Island was −14.7°C and mean summer precipitation was 137 mm, ranging from 72 mm to 208 mm in a period from 1999 to 2005 [*Boike et al.*, 2008]. Frequent cyclones moving through the area cause rapidly changing weather conditions throughout the growing season by advection of cold and moist air from the Arctic Ocean or warm and dry air from continental Siberia, respectively.

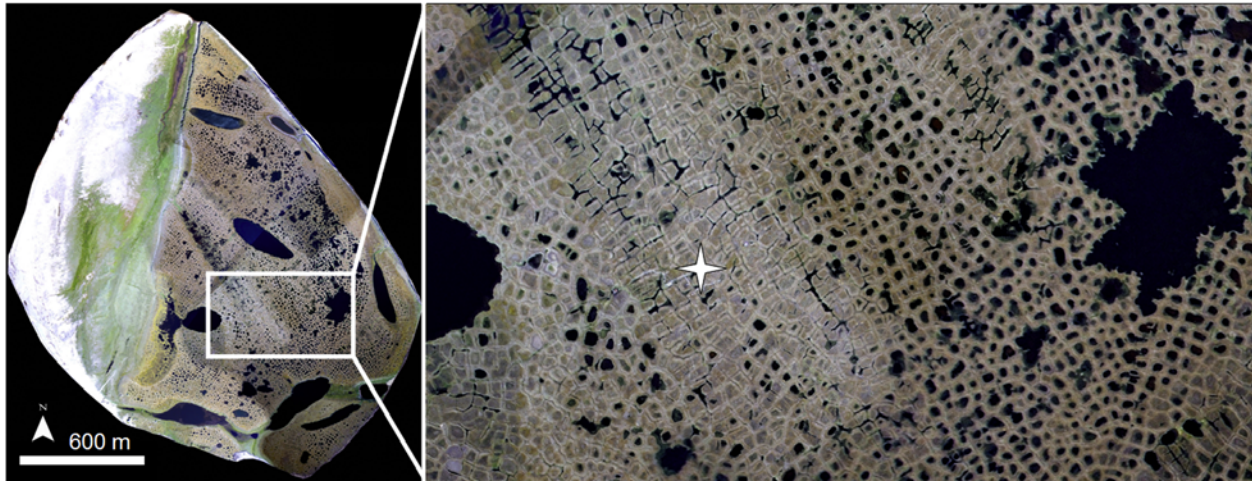


**Figure 2.** Aerial images of the study site. (left) Mosaic of aerial images of Samoylov Island taken in August 2007 (mosaic by Boike *et al.* [2008]). (right) The central part of Samoylov Island in August 2007. The asterisk marks the position of the micrometeorological tower.

Polar day lasts from 7 May to 8 August, and polar night lasts from 15 November to 28 January. Typically, snowmelt and river break up start in the first half of June, and the growing season lasts from mid-June through mid-September. The continuous permafrost in the delta reaches depths of 500 to 600 m [Grigoriev, 1960] and is characterized by very low temperatures between  $-13^{\circ}\text{C}$  and  $-11^{\circ}\text{C}$  [Kotlyakov and Khromova, 2002].

[9] Samoylov Island covers an area of 7.5 km<sup>2</sup> with two main geomorphological units [Kutzbach, 2006]. The western part of the island (3.4 km<sup>2</sup>) is a modern floodplain with elevations from 1 to 5 m above sea level (asl). The study site is located in the center of the eastern part (4.1 km<sup>2</sup>), a Late Holocene river terrace with elevations from 10 to 16 m asl. The surface of the terrace is characterized by wet polygonal tundra. It has a flat macrorelief with slope gradients less than 0.2% except at the shores of larger lakes, where elevation differences of up to 2.5 m occur. However, because of the development of low center ice wedge polygons, the surface is structured by a regular microrelief with typical elevation differences of around 0.5 m between depressed polygon centers and elevated polygon rims. Typical soil types in the poorly drained and hence mostly inundated centers are *Typic Historthels*, while *Glacic* or *Typic Aquiturbels* dominate at the dryer but still moist polygon rims [Soil Survey Staff, 1998; Kutzbach *et al.*, 2004]. In the course of the summer, these soils thaw to a depth of 30 cm to 50 cm.

[10] Hydrophytic sedges such as *Carex aquatilis*, *Carex chondrorrhiza*, and *Carex rariflora* as well as mosses (e.g., *Drepanocladus revolvens*, *Meesia triquetra*, and *Aulacomnium turgidum*) dominate the vegetation in the wet polygon centers and on their edges [Kutzbach *et al.*, 2004; M. Minke, personal communication, 2006]. Mesophytic dwarf shrubs such as *Dryas octopetala* and *Salix glauca*, forbs (*Astragalus frigidus*), and mosses (*Hylocomium splendens*, *Timmia austriaca*) dominate the polygon rims. Surface classification of aerial photographs taken in 2003 shows, that elevated and dryer polygon rims cover approximately 60% of the area surrounding the study site,

while depressed and wet polygon centers and troughs cover 40% of the area (G. Grosse, personal communication, 2005).

### 3. Methods

#### 3.1. Eddy Covariance Setup

[11] The eddy covariance system was set up in the center of the eastern part of Samoylov Island and was surrounded by a relatively homogenous fetch of wet polygonal tundra. Larger lakes were located at the periphery of a 600 m radius around the tower. Successful measurements (i.e., measurements that did not have to be discarded because of technical problems) were conducted on 103 days from 9 June to 19 September 2006, covering an entire growing season from the middle of snowmelt until initial freeze-back.

[12] Wind velocity components and sonic temperature were measured using a three-dimensional sonic anemometer (Solent R3, Gill Instruments Ltd., UK) installed 4 m above ground level. A vacuum pump (RB0021, Busch Inc., Germany) drew sample air at 20 L min<sup>-1</sup> from a sample intake 15 cm below the anemometer measurement point through a CO<sub>2</sub>/H<sub>2</sub>O infrared gas analyzer (LI-7000, LI-COR Inc., USA) and a tunable diode laser spectrometer (TGA 100, Campbell Scientific Ltd., USA) for CH<sub>4</sub> analysis. Before entering the tunable diode laser spectrometer (TDL), sample air was dried in a reversed flow membrane gas dryer (PD-200T-48 SS, Perma Pure Inc., USA). The analyzers and the gas dryer were arranged in series and housed in a temperature-regulated case at the base of the tower. All analog signals were synchronously digitized at 20 Hz and logged on a laptop PC running EdiSol software (J. Massheder, University of Edinburgh, UK). The system was powered by a diesel generator located 100 m southwest from the tower in the least frequent wind direction. An uninterruptible power supply ensured continuous operation.

[13] Additional instruments installed on or near the tower include sensors for air temperature and relative humidity (MP103A, ROTRONIC AG, Switzerland), incoming and

outgoing solar and infrared radiation (CNR1, Kipp and Zonen B.V., The Netherlands), photosynthetically active radiation (QS2, Delta-T Devices Ltd., UK), and barometric pressure (RPT410, Druck Messtechnik GmbH, Germany). Precipitation and soil temperature data were recorded at a long-term monitoring station 700 m south of the eddy covariance tower [Boike *et al.*, 2008]. Additional daily manual measurements at five sites in the footprint of the tower included thaw depth using a steel probe, soil temperatures in 5 cm depth intervals, water level, and soil moisture where no standing water was present. These sites differed with regard to inundation, vegetation, and polygon degradation.

### 3.2. Data Processing

[14] Raw data processing and flux calculation was done using the software EdiRe (R. Clement, University of Edinburgh, UK). Because of relatively low methane fluxes we used an averaging interval of 60 min in order to increase the signal-to-noise ratio of the correlation calculation. Two coordinate rotations were applied to the wind components so that the mean transverse and the mean vertical wind components were reduced to zero. We then removed the time lag between wind measurements at the sonic anemometer and methane concentration measurements in the TDL. The effects of instrument drift and instationary conditions were removed using a recursive high pass filter with a 30 s time constant that was applied to the methane concentration time series. After the initial methane flux calculation, fluxes were corrected for the differences between the flux frequency spectrum and the spectral response of the eddy covariance system, tube attenuation effects, the separation of anemometer and methane analyzer, as well as for the effects of the recursive high pass filter following Moore [1986] and Moncrieff *et al.* [1996]. On average, 35.4% were added to the calculated flux. The correction of the analyzer response accounted for 27.9%, while the high pass filtering of the methane signal accounted for 5.4% of that correction.

[15] The corrected methane flux data were screened thoroughly. Excessively noisy measurements with peaks in the cross-correlation function greater than the flux peak were rejected. We found this procedure to reliably reject measurements which were disturbed for example by instationary conditions, instrument drift, or high wind speeds. Additionally, an integral turbulence characteristics test [Foken and Wichura, 1996] was used for the final screening. The integral turbulence characteristics (ITC) are similarity characteristics of the atmospheric turbulence with a close connection to the correlation coefficient. They characterize whether turbulence is well developed or not, and it is possible to discover some typical effects of nonhomogeneous terrain, such as obstacles or inhomogeneities in surface temperature or moisture conditions [Foken and Wichura, 1996]. Where the ITC parameter deviated more than 30% from the model, the turbulence was assumed to have been disturbed and data were rejected. In total, the screening removed 34.6% of the hourly flux data. However, as we only considered average daily fluxes for all subsequent analyses and there were hourly flux data available for all days (minimum four, average 15), no gap-filling procedures were applied. Measurement errors were estimated using the standard deviation of the cross

correlation function and the average random error was 1.7 mg CH<sub>4</sub> m<sup>-2</sup> d<sup>-1</sup>. Systematic errors for any individual flux measurement have been estimated by Wesely and Hart [1985] to be in the range of 10–20%. The system performance agrees well with the performance other investigators using the TGA 100 have reported and is described in more detail by Wille *et al.* [2008].

[16] The area from which 80% of the cumulative methane flux originated was calculated using a footprint analysis according to Schuepp *et al.* [1990]. The upwind distance of this flux contribution was on average 518 m. The maximum contribution originated from an average distance of 116 m.

### 3.3. Ecosystem-Scale Flux Modeling

[17] We used two approaches to determine flux controlling parameters and set up a small-scale model for the growing period, all of which were based on daily averages of the measured fluxes.

[18] The first approach was purely data based. We used classification and regression tree analysis (CART) as a flexible and robust tool, which can deal with nonlinear relationships, complex interactions, and missing data [Breiman *et al.*, 1984]. Regression trees aim to explain variation in a dependent variable by recursive splitting of the data set into more homogenous subgroups, each of which is characterized by typical values of the dependent variable, the number of data points in the group, and the specific values of the independent variables that define the group. Splitting is continued until an overlarge tree is grown, which is then pruned by cross-validation. We used tenfold cross validation, where the data is divided into ten subsets of approximately equal size, each of which is dropped once in turn while growing a series of trees from the remaining subsets to predict the response of the omitted subset. The estimated error for each subset is summed over all subsets, and after repeating the procedure for each tree size, the tree with the smallest estimated error rate is selected. A more detailed description of this method and its advantages for the exploration, description, and prediction of patterns and processes in ecological data is given by De'ath and Fabricius [2000]. We required a minimum of ten data points in order to allow further splitting and ran a series of 100 tenfold cross validations to select the most frequently occurring tree with the minimum mean squared error.

[19] After identifying the main controls of methane emission, the objective of the second approach was to propose a multiplicative and semideterministic model following the work by Friborg *et al.* [2000], where the flux is a product of an ecosystem reference flux and a set of environmental parameters, each with its specific regulation factor. This approach was also applied by Wille *et al.* [2008], who initially chose parameters for the model on the basis of previously well established relationships, such as the temperature dependence of soil microbial methane production [e.g., Arrhenius, 1909; Conrad, 1989], and on direct correlation between methane flux and the respective parameter. The general form of this model can be written as

$$FCH_4 = a \cdot b^{((T-\bar{T})/10)} \cdot \prod_{i=1}^n f_i(X_i) \quad (1)$$

where  $FCH_4$  is the methane flux time series,  $a$  is the reference flux determined through the fit process,  $b$  is a fit parameter,  $T$  and  $\bar{T}$  are a temperature and reference temperature, respectively, and  $f_i(X_i)$  describe the flux regulation by environmental parameters, where  $f_i$  can be linear or exponential. A weighting factor of  $\sigma_{FCH_4}^{-2}$  was applied to each square of residuals before summing the squares of residuals during the fitting process, with  $\sigma_{FCH_4}$  being the daily mean of the errors of the hourly flux data points.

[20] Models were compared by variance reduction RV, where positive values indicate improvement in model performance. For RV to be significantly different from zero ( $\alpha = 5\%$ ), a required minimum value  $RV_{\min}$  is computed following *Balzer* [1997]:

$$RV_{\min} \approx \frac{186}{(N - 2)^{0.415}} \quad (2)$$

where  $N$  is the number of data points.

## 4. Results

### 4.1. Meteorology

[21] During setup of the instruments at the end of May/beginning of June, the ground around the eddy covariance tower was still mostly snow covered. Only a few snow-free patches occurred on elevated polygon rims. However, mean daily air temperatures were already approaching 0°C and reached 1.5°C on 2 June (Figure 3). Light rainfall starting on 7 June and air temperatures of up to 8.8°C on 6 June and the following days further accelerated snowmelt and by the time continuous measurements started on 9 June, the tundra was almost completely snow free. Thawing of the ice cover on polygonal ponds and thermokarst lakes continued until the end of June, when remaining ice from ponds and smaller lakes that was frozen to the bottom surfaced. After snowmelt, water levels in the polygon centers were more than 11 cm above soil level and slowly decreased throughout June and July to about 2 cm. A storm with precipitation of up to 23 mm per day in the first week of August caused the water levels to rise up to 10 cm above soil level again and they never fell below soil level in the subsequent drying throughout August. Another storm system in the first week of September yielded 34 mm of precipitation within three days causing water levels to rise once more to about 10 cm, where they remained until the end of the measurement period. At a total of 158 mm, liquid precipitation during the study period was above average. Snow started to accumulate on 12 September and reached depths of 8–10 cm in polygon centers and 2–6 cm on elevated areas, but advection of warmer air from the south caused the mean daily air temperature to increase from its minimum at  $-5.3^\circ\text{C}$  on 12 September to  $+4.2^\circ\text{C}$  on 19 September and all snow had disappeared on 18 September. While mean daily air temperature was  $4.5^\circ\text{C}$  during the first half of June and reached a monthly maximum of  $13.0^\circ\text{C}$  on 15 June, soil temperature in a polygon center at 10 cm depth remained slightly below freezing until 14 June. It reached its first of two distinct maxima at  $8.1^\circ\text{C}$  on 11 July, after air temperature had reached daytime maxima of up to  $28.9^\circ\text{C}$  and a

mean daily temperature of  $18.9^\circ\text{C}$ . Soil temperature subsequently declined to about  $5^\circ\text{C}$  until the second peak was reached at  $8.4^\circ\text{C}$  on 2 August, following a second peak in mean daily air temperature of  $18.5^\circ\text{C}$ . From there, soil temperature steadily declined, and refreezing of the soil in 10 cm depth began on 14 September, and on 10 September in the top soil layers, respectively. By mid-September, all water bodies except for the large thermokarst lakes were covered with ice up to 8 cm thick and soils were frozen up to approximately 10 cm depth. The maximum thaw depth of the soil was reached in the beginning of September at 46 cm. The minimum air temperature during the study period was reached at  $-7.2^\circ\text{C}$  on 9 September and the minimum mean daily temperature was  $-3.9^\circ\text{C}$  on 10 September. Despite the high temperatures in July and August, the mean monthly air temperature never exceeded  $10^\circ\text{C}$ . Long-term temperature data are available from Tiksi, which is located 110 km southeast of Samoylov Island but characterized by very similar temperatures. Temperature conditions in 2006 were almost  $5^\circ\text{C}$  warmer than the long-term average in June ( $2^\circ\text{C}$ ) but within  $\pm 1^\circ\text{C}$  of the long-term average in July ( $7^\circ\text{C}$ ), August ( $7^\circ\text{C}$ ), and September ( $1^\circ\text{C}$ ). The average daily wind speed was  $5.1 \text{ m s}^{-1}$  during the study period, which is  $0.4 \text{ m s}^{-1}$  higher than in 2003 and 2004 [*Kutzbach*, 2006]. Winds from east-southeast were clearly predominant, but west-northwesterly and southern winds also occurred frequently (data not shown).

### 4.2. Ecosystem-Scale Methane Flux

[22] Mean daily methane flux was  $18.7 \text{ mg m}^{-2} \text{ d}^{-1}$  during the study period and showed relatively small seasonal variation (Figure 3). However, strong variations could be observed, which coincided with pronounced decreases in air pressure, higher wind speed after calm periods, and precipitation events.

[23] In the first two weeks of measurements, average daily methane fluxes were already  $13.8 \text{ mg m}^{-2} \text{ d}^{-1}$ , with high variability from  $5.7 \text{ mg m}^{-2} \text{ d}^{-1}$  to  $22.0 \text{ mg m}^{-2} \text{ d}^{-1}$ . Soil temperature was still below  $0^\circ\text{C}$  when measurements started and showed very little variation in the early part of the thawing period. The lowest methane flux was observed during days with relatively high air pressure and low wind speed. Methane fluxes increased to an average of  $25.0 \text{ mg m}^{-2} \text{ d}^{-1}$  in the third week; however, this increase was mainly due to an extreme peak on 27 June, which coincided with the lowest observed air pressure during the summer and high wind speeds. The last ice from the bottom of ponds and smaller lakes surfaced and melted around this time.

[24] Methane fluxes dropped to an average of  $12.3 \text{ mg m}^{-2} \text{ d}^{-1}$  during the calm period at the end of June, and then steadily increased to the highest measured fluxes of on average  $35.1 \text{ mg m}^{-2} \text{ d}^{-1}$  in the first week of August, roughly following variations in soil temperature and closely following variations in wind speed. Throughout July, above-average methane fluxes frequently correlated with sudden decreases in air pressure. Until the third week of August, fluxes remained between  $17.0$  and  $20.0 \text{ mg m}^{-2} \text{ d}^{-1}$  and then decreased to less than  $13.0 \text{ mg m}^{-2} \text{ d}^{-1}$  during a longer calm high-pressure period at the end of August.

[25] During the first and second week of September, which were characterized by rapidly decreasing air pres-

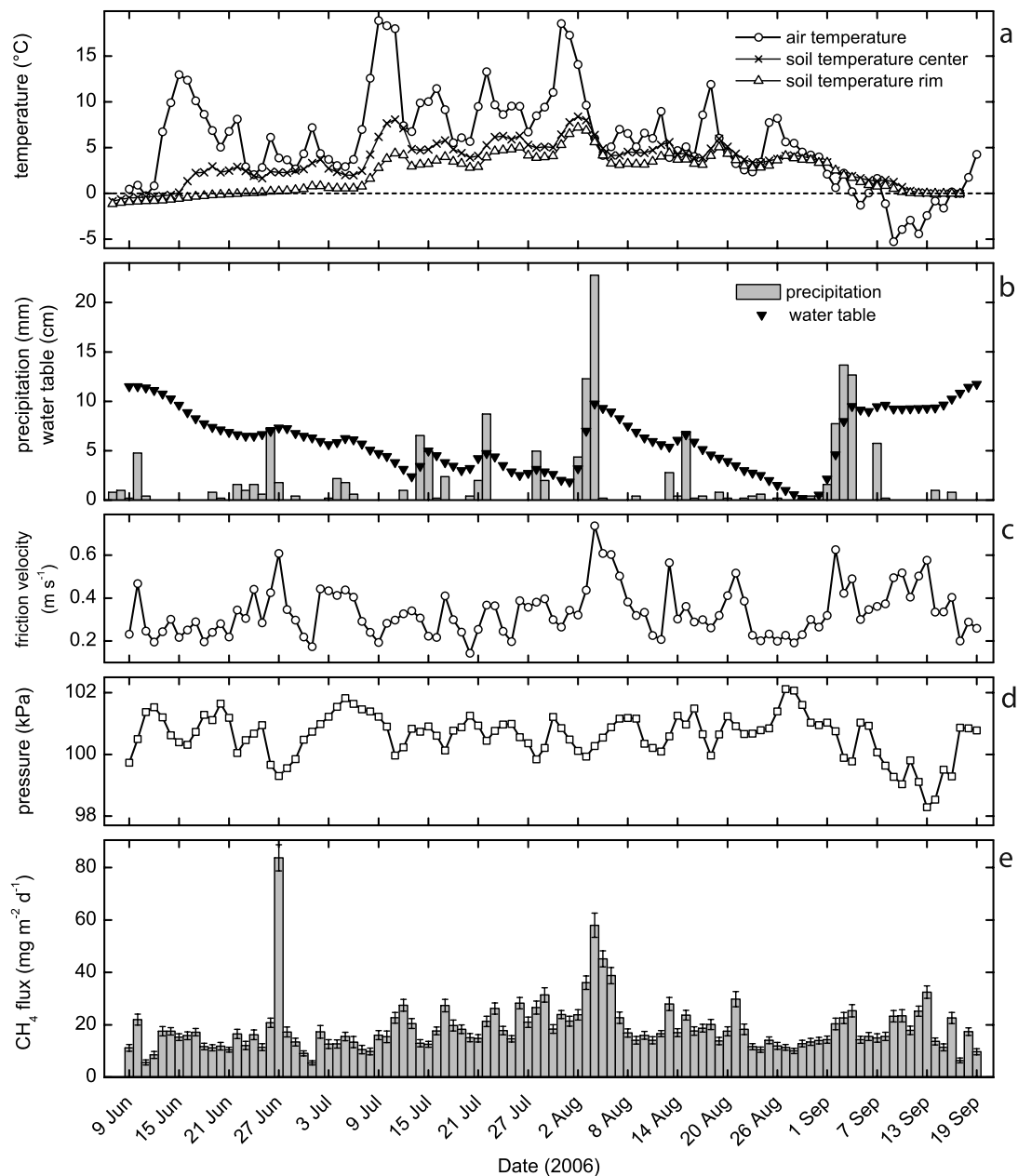


**Figure 3.** Data of the 2006 growing season. (a) Air temperature at 2 m above surface, soil temperature at a polygon center in 0.10 m depth, and soil temperature at a polygon rim in 0.20 m depth; (b) liquid precipitation and water table relative to the soil surface in a polygon center; (c) friction velocity  $u_*$ ; (d) atmospheric pressure; and (e) methane flux as measured by eddy covariance (Error bars denote the average random error.). All data are shown as daily means.

sure, partly strong winds, and rain or snow events, methane fluxes increased to an average of  $18.2 \text{ mg m}^{-2} \text{ d}^{-1}$  and  $21.6 \text{ mg m}^{-2} \text{ d}^{-1}$ , respectively, despite a decrease in soil temperature and refreezing of the top soil layers and water bodies. By mid-September, all water bodies except for the large thermokarst lakes where covered with ice up to 8 cm thick. During the calm high-pressure period after 13 September, methane fluxes decreased markedly to below  $10.0 \text{ mg m}^{-2} \text{ d}^{-1}$  at the end of the measurement period.

[26] Classification and regression tree analysis (CART) of the measured methane flux data and environmental variables showed that variation in methane fluxes could best be explained by friction velocity  $u_*$  and soil temperatures at 10 cm depth in a polygon center and 20 cm depth in a polygon rim, respectively. Friction velocity alone accounted for 57% of the variance in methane emissions and another 3% could be explained by wind speed, which is closely correlated with friction velocity and its main surrogate variable in the CART analysis. Soil temperatures on the other hand only explained about 8% of the variance (Figure 4). This

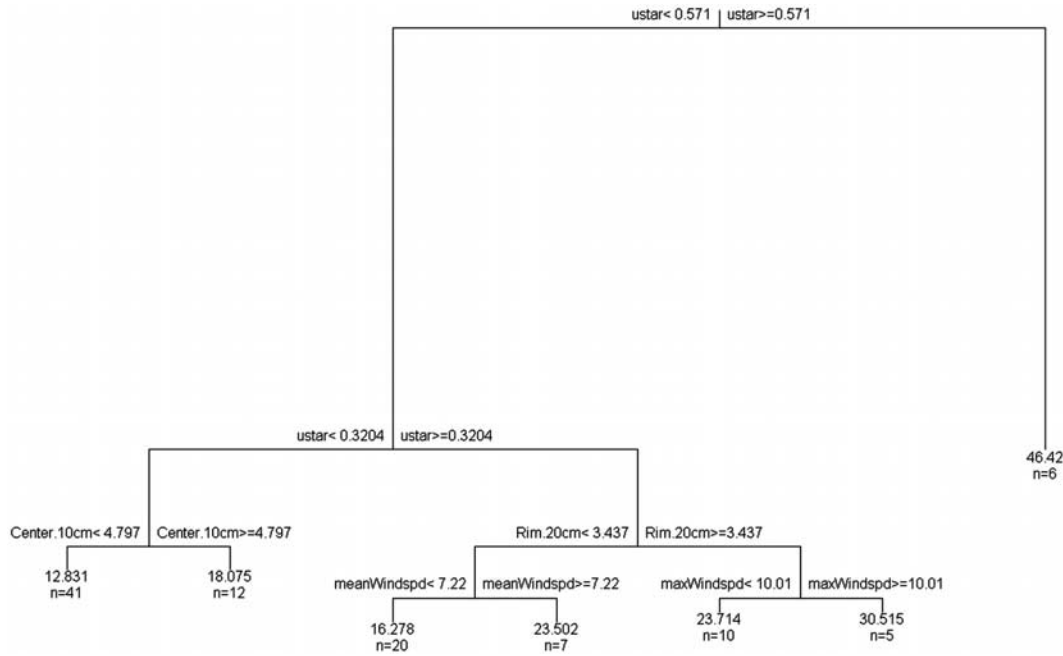


**Figure 4.** Regression tree determined by 100 tenfold cross validations and pruning to the level of the smallest mean square error. The most frequently occurring tree was selected. The label at each split denotes the splitting criterion (the first split here is at  $u_* = 0.571 \text{ m s}^{-1}$ ), and the labels at the “leaves” of the tree indicate the number of data points  $n$  in the respective “leaf” as well as the mean of the respective data points. Near-surface turbulence (friction velocity  $u_*$ ) explains most of the variability in methane emissions through the first two splits. In the next two splits, a considerably smaller amount of variability is explained by soil temperatures in a polygon center at 10 cm depth and in a polygon rim at 20 cm depth. In the final splits, more variability is explained by atmospheric parameters, i.e., by mean horizontal wind speed  $u$ , which directly correlates with  $u_*$ , and by maximum horizontal wind speed. Terminal nodes are labeled with means of the respective variable and the number of observations in the subgroup.

combination of  $u_*$  and  $T$  conformed to the model proposed by *Wille et al.* [2008] using the following equation:

$$\text{FCH}_4 = a \cdot b^{((T-\bar{T})/10)} \cdot c^{(u^*-\bar{u}^*)}, \quad (3)$$

where  $T$  is the soil temperature at a depressed polygon center in 20 cm depth,  $u_*$  is the friction velocity, and  $\bar{T}$  and  $\bar{u}_*$  are the mean values of the respective variables. Applying this model with the fit parameters determined by *Wille et al.* [2008] (Table 1) to the data of the 2006 measurement period explained only about 40% of the variance seen in the flux data and tended to overestimate fluxes larger than  $25 \text{ mg m}^{-2} \text{ d}^{-1}$  while underestimating some of the lower fluxes (Figure 5). It also did not adequately capture variation in methane fluxes associated with decreases in air pressure that could be seen

throughout July. Model performance was improved by using a soil temperature at 10 cm depth in a polygon center, where methane production takes place, as identified by CART and renewed fitting; however, the best agreement ( $R^2_{\text{adj}} = 0.68$ ; Table 1) of modeled and measured data was obtained by expanding the model proposed by *Wille et al.* [2008] with an exponential term that accounts for the observed influence of air pressure:

$$\text{FCH}_4 = a \cdot b^{((T-\bar{T})/10)} \cdot c^{(u^*-\bar{u}^*)} \cdot d^{(p-\bar{p})}, \quad (4)$$

where  $T$  is the soil temperature at 10 cm depth in a polygon center,  $u_*$  is the friction velocity,  $p$  is the air pressure, and  $\bar{T}$ ,  $\bar{u}_*$ , and  $\bar{p}$  are the mean values of the respective variables.

**Table 1.** Input and Fit Parameters for the Model Proposed Here (Equation (4)) and the Model Proposed by *Wille et al.* [2008] (Equation (3))<sup>a</sup>

Model	$\bar{T}$ (°C)	$\bar{u}_*$ (m s <sup>-1</sup> )	$\bar{p}$ (kPa)	$a$ (mg m <sup>-2</sup> d <sup>-1</sup> )	$b$	$c$	$d$	$R^2$	$R^2_{\text{adj}}$	RV (%)
This paper	3.44	0.34	100.617	$16.68 \pm 0.16$	$2.28 \pm 0.10$	$11.16 \pm 0.94$	$0.86 \pm 0.01$	0.69	0.68	33.07
This paper (excluding pressure)	3.44	0.34	-	$16.79 \pm 0.16$	$2.07 \pm 0.09$	$14.41 \pm 1.12$	-	0.63	0.62	18.07
<i>Wille et al.</i> [2008]	1.94	0.28	-	$15.67 \pm 0.46$	$3.93 \pm 0.50$	$25.26 \pm 7.23$	-	0.40	0.39	-

<sup>a</sup> $R^2_{\text{adj}}$  is the adjusted  $R^2$  taking into consideration the number of explanatory variables. Models were compared to the model proposed by *Wille et al.* [2008] using variance reduction RV, where positive values indicate improvement in model performance. For RV to be significantly different from zero ( $\alpha = 5\%$ ), a minimum value of  $\text{RV}_{\text{min}} = 27.40\%$  was calculated using equation (2). The extended model proposed here is significantly better than the model proposed by *Wille et al.* [2008].

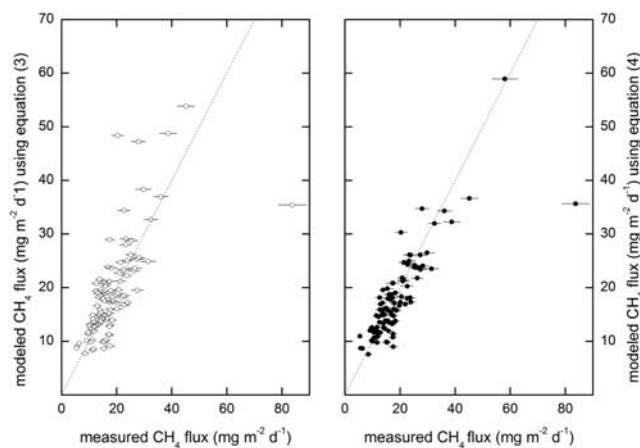


**Figure 5.** Modeled flux versus mean daily flux. (left) Using the model as proposed by *Wille et al.* [2008] (equation (3)), larger fluxes are overestimated. (right) Using the extended model proposed here (equation (4)), fluxes agree well over the entire range of fluxes.

[27] Thaw depth, which increased gradually and without variation throughout the season, did not improve the model, and neither did water level, which remained above the soil surface at all times in the polygon centers.

[28] While fluxes modeled using equation (4) agreed well with measured fluxes, Figure 6 shows that measured fluxes during the thaw period, when soil temperature variation was low, were underestimated. Also, less than 50% of the actual methane emission on 27 June could be modeled using either of the approaches described above. Substituting air temper-

ature for soil temperature in equation (4) does not significantly improve the model as a whole, but underestimation of fluxes during the thaw period was reduced substantially (Figure 6).

[29] The cumulative methane emission during the 2006 growing season was  $1.93 \text{ g m}^{-2}$ , which agrees well with the cumulative flux during the same period of a combined 2003 and 2004 data set, which amounted to  $1.87 \text{ g m}^{-2}$  [*Wille et al.*, 2008]. The extended model (equation (4)) underestimated the cumulative measured flux by less than 5%.

## 5. Discussion

### 5.1. Environmental Controls on Methane Emission

[30] To our best knowledge, we here present the first ecosystem-scale methane exchange data from the Siberian Arctic covering an entire contiguous growing season from spring thaw to initial freeze-back by the eddy covariance method. The measurement period included a wide range of meteorological and soil conditions, allowing for a comprehensive analysis of the environmental controls of methane fluxes. The most important parameter controlling methane emissions from our site was near-surface turbulence, which closely correlates with horizontal wind speed. Though few other studies have reported this effect, our results confirm the conclusions by *Wille et al.* [2008], who observed the same relationship during a “synthetic” growing season of 2003/2004 eddy covariance data from the same site (Table 1). *Fan et al.* [1992] found emissions from lakes in Alaskan Arctic tundra to be dependent on wind speed and *Hargreaves et al.* [2001] described a close relationship between momentum flux and methane emissions for short periods of up to one day at a tundra site in Finnish Lapland.

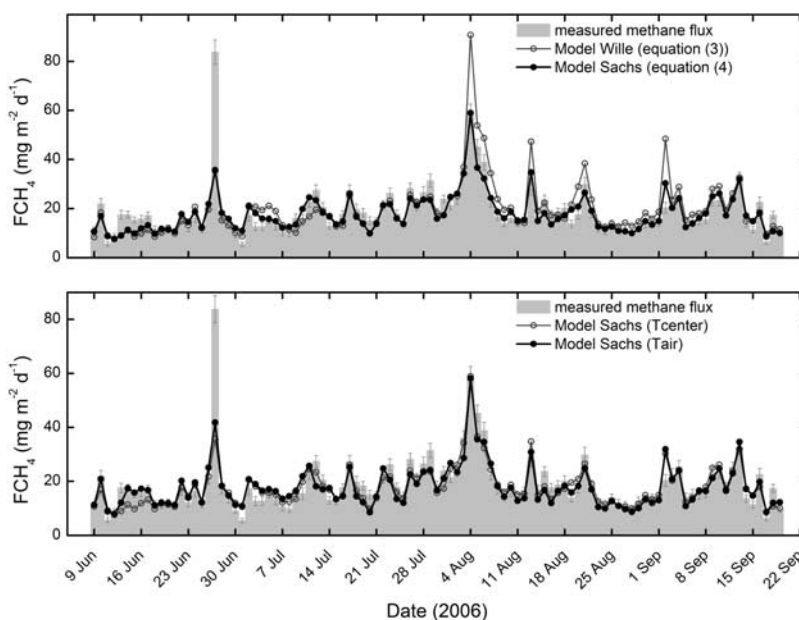


**Figure 6.** Time series of measured and modeled daily mean CH<sub>4</sub> fluxes. (top) Fluxes modeled using equations (3) and (4). The model by *Wille et al.* [2008] tends to overestimate larger methane fluxes. (bottom) Fluxes modeled using equation (4) and a modified version of equation (4), where soil temperature in 10 cm depth was replaced by 2 m air temperature. The underestimation of methane fluxes during the early thaw period is reduced substantially.

The concurrent observation of ebullition in the latter study indicates a water table above the soil surface. Our site features a large fraction of polygon centers with water tables above the surface, deep thermokarst cracks, and small polygonal ponds of various depths. Thus the methane flux dependence on near-surface turbulence could at least partly be explained by diffusive and turbulent gas transfer between water surface and atmosphere, which several lake studies have shown to be proportional to  $u^{1.6}$ , with  $u$  being the horizontal wind speed [MacIntyre *et al.*, 1995].

[31] Increased turbulence and wind speed on noninundated surfaces such as polygon rims and, probably more so, high center polygons, which are dominated by thick moss layers, could lead to a thinning of the laminar boundary layer in the moss canopy, resulting in a higher concentration gradient from the methane-enriched soil to the turbulent boundary layer and hence to an increased diffusive flux of methane. In addition, increased turbulence could lead to increased aeration and a transient flushing of methane stored in these layers during calm periods. Increased methane emissions during high wind speeds after calm periods were also reported by Hargreaves *et al.* [2001]. However, this storage flushing is of highly transient nature and thus might only play a role on shorter timescales.

[32] Another important mechanism for methane emissions from lakes and water inundated areas is bubble ebullition, which is often ignored because of its patchiness and resulting difficulties in quantifying it. Hargreaves *et al.* [2001] have observed ebullition during spring thaw and periods of high wind speed. Walter *et al.* [2006] reported methane release by ebullition from eastern Siberian thermokarst lakes, which was continuous and large enough to prevent some emission hot spots in the investigated lakes from freezing. During closed chamber flux measurements in close proximity to the eddy covariance tower, we captured ebullition events using floating chambers on thermokarst cracks (data not shown) and repeatedly observed ebullition from polygonal ponds during the thawing period. We suggest two main triggers for methane ebullition: (1) increased atmospheric turbulence and (2) decreased atmospheric pressure. Increased turbulence could lead to the release of gas bubbles that adhere to surfaces below the water table, such as plants, roots, or shallow sediments through wind induced turbulence in the water, agitation of plants, or wave action. Decreasing atmospheric pressure, which frequently correlated with increased methane emission from our study site, can release free-phase gas and resulting ebullition was shown to contribute 50–64% to total emissions reported from a Japanese peatland by Tokida *et al.* [2007]. Laboratory experiments by Tokida *et al.* [2005] also demonstrated the importance of atmospheric pressure on methane ebullition, and including the pressure term in our model (equation (4)) improved model performance significantly (Table 1).

[33] Soil temperature in a polygon center at 10 cm depth was identified as the third parameter controlling methane fluxes from our site. The dependence of soil microbial activity on temperature was already described almost a century ago by Arrhenius [1909] and has been confirmed by several studies since [e.g., Conrad, 1989; Hargreaves

*et al.*, 2001; Christensen *et al.*, 2001]. However, while Hargreaves *et al.* [2001] found a very strong relationship between methane emission and peat temperature, Rinne *et al.* [2007] for example, found a good exponential relationship only for temperatures  $<12^{\circ}\text{C}$ . Other studies, such as Wickland *et al.*'s [2006], did not find a relationship between methane emission and soil temperature. At our study site, we found soil temperature to play a minor role, explaining 8% of the observed methane fluxes. However, during spring thaw, substituting air temperature for soil temperature resulted in a better model fit and reduced the underestimation of early season methane fluxes. This is considered to be due to the fact, that deeper soil layers were still frozen and most of the methane emitted during that early phase originated from methanogenesis in the uppermost soil layers and from release of trapped methane from lake ice and ponds. Temperatures in these sources are likely to be directly influenced by air temperature rather than soil temperature in several centimeters depth. Increased temperature would increase melt/thaw rates, resulting in higher emissions of stored methane.

[34] Some studies do not separate methane production or even potential microbial activity from actual methane release [e.g., Wagner *et al.*, 2003]. However, the clear dominance of atmospheric parameters over soil temperature found here has two main implications:

[35] 1. It suggests that methane production and methane emission are not necessarily closely linked, particularly on shorted timescales. Instead, storage of methane in soils and sediments leads to a certain degree of decoupling between temperature-dependent methane production and meteorology-dependent methane release. Light disturbance of sediments underneath a floating chamber using a steel probe resulted in rapid fivefold increase of the methane concentration inside the chamber, suggesting that large amounts of free-phase methane are stored in sediments of polygon ponds and lakes as well as thermokarst cracks.

[36] 2. When measuring gas exchange by the closed chamber method, near-surface turbulence and, depending on chamber design, also air pressure are inherently eliminated, while many other parameters including air and soil temperature are altered inside the chamber [Kutzbach *et al.*, 2007]. As most studies on the quantification and source strengths of methane emissions (including those that upscale emission estimates to the landscape or regional scale) are currently based on closed chamber methods, this finding raises questions about the reliability of reported field data based on chamber measurements and highlights the need for studies based on nonintrusive measurement techniques such as the eddy covariance approach.

[37] While other studies found thaw depth to be correlated with methane emission [Friborg *et al.*, 2000; van Huissteden *et al.*, 2005], we did not find a significant influence of thaw depth on methane emission at our site, confirming the findings discussed by Wille *et al.* [2008].

[38] As methane is produced under anaerobic conditions in the soil column and oxidized under aerobic conditions, water table depth is another variable, which has often been identified as predictor for methane emissions [e.g., Friborg *et al.*, 2000; Suyker *et al.*, 1996]. However, Rinne *et al.* [2007] found only a weak anticorrelation between methane

emission and water table position, and *Hargreaves et al.* [2001] did not find any relationship between these parameters. At our site, we did not find any relationship between ecosystem-scale methane emission and water table position. However, simultaneous closed chamber measurements on fifteen plots at five different microsites in close proximity to the eddy covariance tower showed a high small-scale variability of methane fluxes between sites with low water tables (i.e., polygon rims and high center polygons) and sites with water tables near the surface (i.e., polygon centers). While emissions from rim and high center polygon plots frequently did not reach/exceed the detection limit of the analyzer, large fluxes of up to 400 mg m<sup>-2</sup> d<sup>-1</sup> were measured in inundated polygon centers (data not shown). Since the water table in these polygon centers never dropped below the soil surface and precipitation quickly drained from elevated polygon rims into polygon centers, there were no significant temporal changes in the ratio of aerobic and anaerobic areas in the soil column and thus no temporal changes in methane emission related to water table position.

## 5.2. Seasonal Dynamics

[39] Although soils were still frozen at the beginning of the 2006 measurement period, substantial methane emission could already be observed, confirming the observations from the same site in 2004 [*Willie et al.*, 2008]. These early emissions were highly variable and dependent on atmospheric conditions. The highest emission peak of the entire season was observed on 27 June, toward the end of the thawing period. *Rinne et al.* [2007] also reported an emission pulse during snowmelt, which was independent of soil temperature. *Hargreaves et al.* [2001] found methane fluxes in the range of summer emissions during the thaw period, which were attributed to the release of methane trapped in and below the ice cover. *Harazono et al.* [2006] on the other hand, did not observe an increase in methane emission during spring thaw at a wet tundra site in Barrow, Alaska.

[40] Visual observation of ebullition from thawing lake shores and lake ice suggests that this pathway played a major role in early methane emission on Samoylov Island. The large emission peak on 27 June coincided with the end of the thawing period, when remaining ice from ponds and lakes, which were frozen solid, broke loose from the lake bottoms and surfaced, presumably disturbing bottom sediments and thus causing free-phase methane to be released. In addition, through the processes described above, strong winds and a pronounced drop in air pressure might have caused unusual high emission of methane produced and stored during the winter.

[41] Monthly average methane fluxes of 17.1 mg m<sup>-2</sup> d<sup>-1</sup> in June, 18.3 mg m<sup>-2</sup> d<sup>-1</sup> in July, 20.6 mg m<sup>-2</sup> d<sup>-1</sup> in August, and 18.2 mg m<sup>-2</sup> d<sup>-1</sup> in September agree well with fluxes from the same site reported by *Wille et al.* [2008]. Emissions are similar to the average methane flux reported by *Fan et al.* [1992] from an Alaskan subarctic tundra site, which was characterized by a mix of dry and wet microsites as well as lakes with a ratio of wet/dry sites comparable to Samoylov Island. The other eddy covariance flux studies from Arctic sites reported higher fluxes. *Friborg et al.* [2000] reported August methane fluxes of 50 mg m<sup>-2</sup> d<sup>-1</sup> from a rich fen near Zackenberg (Greenland), *Hargreaves et al.*

[2001] measured emissions of typically 38 mg m<sup>-2</sup> d<sup>-1</sup> from a wetland in Finnish Lapland, and *Harazono et al.* [2006] reported methane fluxes from a coastal wet sedge tundra in Barrow, Alaska, of  $\geq 50$  mg m<sup>-2</sup> d<sup>-1</sup> until the end of August. However, all these sites have a considerably larger fraction of wet or inundated surfaces than our site on Samoylov Island, where relatively dry polygon rims make up about 60% of the surface area. Thus, less than half the area covered by the eddy covariance footprint actually contributes significant methane emissions. In addition, extremely cold permafrost in northern Siberia might inhibit microbial activity. Methanogenesis is also impeded by unfavorable conditions, such as sandy soils and substrate limitation because of only weakly decomposed organic matter [*Ganzert et al.*, 2006].

[42] Relatively high fluxes could also be observed in September. However, with the top soil layer frozen and water bodies covered by up to 8 cm of ice, these high fluxes are harder to explain by turbulence or atmospheric pressure influence, especially in the last two weeks of measurements. The remaining pathway for methane emission while soil and water bodies freeze from the top, is via plant mediated transport through the aerenchyma of wet-adapted aerenchymatous sedges and grasses such as *Carex aquatilis*, which was shown to account for 27% to 66% of overall methane fluxes on Samoylov Island [*Kutzbach et al.*, 2004]. However, this study also suggested that plant-mediated transport was only driven by diffusion and presumably limited by the diffusion resistance of dense root exodermes, leading *Wille et al.* [2008] to hypothesize that near-surface turbulence is not likely to increase methane emission via this pathway. However, in light of the 2006 data this should be qualified as the diffusion resistance of the root exodermes has not been quantified and the correlations between increased turbulence and methane emission, and decreasing atmospheric pressure and methane emission were still apparent during refreezing of soil and water bodies. Similar to the effect of increased aeration in moss canopies, higher wind speed and lower atmospheric pressure would decrease the aerodynamic resistance in the turbulent boundary layer and the thickness of the laminar boundary layer at the leaf surfaces, thus allowing the diffusion from aerenchyma to the atmosphere to increase.

[43] In addition, incidental observations in the field indicate that refreezing of the top soil pressurizes the unfrozen layer underneath, possibly forcing increased emission from unfrozen patches or through cracks. These increased emissions could result from the added effect the freezing has on two usually opposing processes: (1) it limits the transportation of oxygen from the atmosphere to the soil, thus promoting the net formation of methane in the unfrozen layers [*Yu et al.*, 2007], and (2) it early on reduces methane consumption in the freezing upper layers, as methane oxidizing bacteria in these layers were found to have a higher temperature optimum [*Liebner and Wagner*, 2007] and thus reduce their activity earlier than the psychrotolerant methanogens in the still unfrozen lower horizons [*Ganzert et al.*, 2006]. Hence, an increased net amount of methane is available for emission.

[44] However, the poorly understood effects of freezing-induced structural properties of cold soils on methane transport processes and pathways, and the lack of ecosystem-scale data on cold season methane fluxes highlight the

need for long-term nonintrusive studies, which extend well beyond the growing season.

## 6. Conclusions

[45] In comparison to three other Arctic eddy covariance studies from Alaska, Greenland, and Finland, methane emission was low at our site, probably because of (1) extremely cold permafrost, (2) substrate limitation of the methanogens, and (3) a relatively high surface coverage of noninundated, moderately moist areas.

[46] Near-surface turbulence was identified as the most important control on ecosystem-scale methane emission, while soil temperature explained only 8% of the seasonal emission. In addition, atmospheric pressure was found to significantly improve a model based on turbulence and soil temperature.

[47] Ebullition from waterlogged areas triggered by falling atmospheric pressure and near-surface turbulence is thought to be an important pathway that warrants more attention in future studies. In this context, available free-phase gas in lake and thermokarst crack sediments should be quantified in order to estimate potential emissions by ebullition.

[48] The close coupling of methane fluxes and atmospheric parameters demonstrated here raises questions regarding the reliability of enclosure-based measurements, which inherently exclude these parameters. Long-term, nonintrusive measurements on the ecosystem scale are needed to adequately quantify high-latitude methane emissions and correct potentially biased estimates based on chamber measurements, to identify processes governing the emission of methane on various scales, and to address interannual and long-term variations of methane emission from a range of Arctic ecosystems.

[49] **Acknowledgments.** We would like to thank the members of the joint Russian-German expedition LENA-2006, especially Waldemar Schneider (Alfred Wegener Institute), Dmitry Yu. Bolshianov (Arctic and Antarctic Research Institute, St. Petersburg), Mikhail N. Grigoriev (Permafrost Institute, Yakutsk), Alexander Y. Derevyagin (Moscow State University), and Dmitri V. Melnitschenko (Hydro Base, Tiksi) for all logistical, travel, and administrative arrangements. We are also grateful to Günther “Molo” Stooft for technical support in the field. We greatly appreciate support from Eva-Maria Pfeiffer, Barnim Thees, Sina Muster, and Merten Minke on various aspects of this study, as well as thoughtful comments from two reviewers that helped improving the manuscript. This work was conducted in the frame of the Helmholtz Integrated Earth Observing System (Helmholtz-EOS) Ph.D. program.

## References

- Are, F. E., and E. Reimnitz (2000), An overview of the Lena River Delta setting, geology, tectonics, geomorphology, and hydrology, *J. Coastal Res.*, *16*(4), 1083–1093.
- Arrhenius, S. (1909), *Theorien der Chemie, Nach Vorlesungen gehalten an der Universität von Kalifornien zu Berkeley*, 2nd ed., Akademische, Leipzig, Germany.
- Balzer, K. (1997), Mindest RV, Beitrag zum Langfristprognoseseminar beim Gemeinsamen Seminar am Institut für Meteorologie der FU, FU Berlin, Germany.
- Boike, J., C. Wille, and A. Abnizova (2008), The climatology, and summer energy and water balance of polygonal tundra in the Lena River Delta, Siberia, *J. Geophys. Res.*, doi:10.1029/2007JG000540, in press.
- Breiman, L., J. H. Friedman, R. A. Olshen, and C. J. Stone (1984), *Classification and Regression Trees, Wadsworth Statistics/Probability Series*, CRC Press, Boca Raton, Fla.
- Cao, M., S. Marshall, and K. Gregson (1996), Global carbon exchange and methane emissions from natural wetlands: Application of a process-based model, *J. Geophys. Res.*, *101*(D9), 14,399–14,414, doi:10.1029/96JD00219.
- Chapin, F. S., III, et al. (2000), Arctic and boreal ecosystems of western North America as components of the climate system, *Global Change Biol.*, *6*, 211–223, doi:10.1046/j.1365-2486.2000.06022.x.
- Christensen, T. R., S. Jonasson, T. V. Callaghan, and M. Havström (1995), Spatial variation in high-latitude methane flux along a transect across Siberian and European tundra environments, *J. Geophys. Res.*, *100*(D10), 21,035–21,046, doi:10.1029/95JD02145.
- Christensen, T. R., I. C. Prentice, J. Kaplan, A. Haxeltine, and S. Sitch (1996), Methane flux from northern wetlands and tundra: An ecosystem source modelling approach, *Tellus, Ser. B*, *48*, 652–661.
- Christensen, T. R., T. Friborg, M. Sommerkorn, J. Kaplan, L. Illeris, H. Soegaard, C. Nordstroem, and S. Jonasson (2000), Trace gas exchange in a high-arctic valley 1. Variations in CO<sub>2</sub> and CH<sub>4</sub> flux between tundra vegetation types, *Global Biogeochem. Cycles*, *14*(3), 701–714, doi:10.1029/1999GB001134.
- Christensen, T. R., D. Lloyd, B. Svensson, P. J. Martikainen, R. Harding, H. Oskarsson, H. Soegaard, T. Friborg, and N. Panikov (2001), Biogenic controls on trace fluxes in northern wetlands, *IGBP Global Change Newsl.*, *51*, 9–15.
- Conrad, R. (1989), Control of methane production in terrestrial ecosystems, in *Exchange of Trace Gases between Terrestrial Ecosystems and the Atmosphere*, edited by M. O. Andreae and D. S. Schimel, pp. 39–58, John Wiley, Chichester, U.K.
- Corradi, C., O. Kolle, K. Walter, S. A. Zimov, and E.-D. Schulze (2005), Carbon dioxide and methane exchange of a north-east Siberian tussock tundra, *Global Change Biol.*, *11*, 1910–1925, doi:10.1111/j.1365-2486.2005.01023.x.
- De'ath, G., and K. E. Fabricius (2000), Classification and regression trees: A powerful yet simple technique for ecological data analysis, *Ecology*, *81*(11), 3178–3192.
- Fan, S. M., S. C. Wofsy, P. S. Bakwin, D. J. Jacob, S. M. Anderson, P. L. Keibian, J. B. McManus, C. E. Kolb, and D. R. Fitzjarrald (1992), Micrometeorological measurements of CH<sub>4</sub> and CO<sub>2</sub> exchange between the atmosphere and subarctic tundra, *J. Geophys. Res.*, *97*(D15), 16,627–16,643.
- Foken, T., and B. Wichura (1996), Tools for quality assessment of surface-based flux measurements, *Agric. For. Meteorol.*, *78*(1–2), 83–105, doi:10.1016/0168-1923(95)02248-1.
- Friborg, T., T. R. Christensen, B. U. Hansen, C. Nordstroem, and H. Soegaard (2000), Trace gas exchange in a high-arctic valley 2. Landscape CH<sub>4</sub> fluxes measured and modeled using eddy correlation data, *Global Biogeochem. Cycles*, *14*(3), 715–724, doi:10.1029/1999GB001136.
- Friborg, T., H. Soegaard, T. R. Christensen, C. R. Lloyd, and N. S. Panikov (2003), Siberian wetlands: Where a sink is a source, *Geophys. Res. Lett.*, *30*(21), 2129, doi:10.1029/2003GL017797.
- Fung, I., J. John, J. Lerner, E. Matthews, M. Prather, L. P. Steele, and P. J. Fraser (1991), Three-dimensional model synthesis of the global methane cycle, *J. Geophys. Res.*, *96*(D7), 13,033–13,065, doi:10.1029/91JD01247.
- Ganzert, L., G. Jurgens, U. Münster, and D. Wagner (2006), Methanogenic communities in permafrost-affected soils of the Laptev Sea coast, Siberian Arctic, characterized by 16S rRNA gene fingerprints, *FEMS Microbiol. Ecol.*, *59*(2), 476–488, doi:10.1111/j.1574-6941.2006.00205.x.
- Grigoriev, N. F. (1960), The temperature of permafrost in the Lena Delta basin-Deposit conditions and properties of the permafrost in Yakutia (in Russian), *Yakutsk*, *2*, 97–101.
- Harazono, Y., M. Mano, A. Myiata, M. Yoshimoto, R. C. Zulueta, G. L. Vourlitis, H. Kwon, and W. C. Oechel (2006), Temporal and spatial differences of methane flux at arctic tundra in Alaska, Mem, *Natl. Inst. Polar Res. Spec. Issue Jpn.*, *59*, 79–95.
- Hargreaves, K. J., D. Fowler, C. E. R. Pitcairn, and M. Aurela (2001), Annual methane emission from Finnish mires estimated from eddy covariance campaign measurements, *Theor. Appl. Climatol.*, *70*, 203–213, doi:10.1007/s007040170015.
- Hubberten, H.-W., D. Wagner, E.-M. Pfeiffer, J. Boike, and A. Y. Gukov (2006), The Russian-German research station Samoylov, Lena Delta-A key site for polar research in the Siberian Arctic, *Polarforschung*, *73*(2/3), 111–116.
- Intergovernmental Panel on Climate Change (2001), *Climate Change 2001: The Scientific Basis: Contribution of Working Group I to the Third Assessment Report of the Intergovernmental Panel on Climate Change*, edited by J. T. Houghton et al., 944 pp., Cambridge Univ. Press, New York.
- Kotlyakov, V., and T. Khromova (2002), Permafrost, snow and ice, in *Land Resources of Russia* [electronic], edited by V. Stolbovoi and I. McCallum, Int. Inst. Appl. Syst. Anal. Russ. Acad. Sci., Laxenburg, Austria.
- Kutzbach, L. (2006), The exchange of energy, water and carbon dioxide between wet arctic tundra and the atmosphere at the Lena River Delta,

- Northern Siberia, in *Reports on Polar and Marine Research, Rep. 541*, 157 pp., Alfred Wegener Inst., Bremerhaven, Germany.
- Kutzbach, L., D. Wagner, and E.-M. Pfeiffer (2004), Effect of microrelief and vegetation on methane emission from wet polygonal tundra, Lena Delta, Northern Siberia, *Biogeochemistry*, *69*, 341–362, doi:10.1023/B:Biog.0000031053.81520.db.
- Kutzbach, L., J. Schneider, T. Sachs, M. Giebels, H. Nykänen, N. J. Shurpali, P. J. Martikainen, J. Alm, and M. Wilmking (2007), CO<sub>2</sub> flux determination by closed-chamber methods can be seriously biased by inappropriate application of linear regression, *Biogeosciences*, *4*, 1005–1025.
- Liebner, S., and D. Wagner (2007), Abundance, distribution and potential activity of methane oxidizing bacteria in permafrost soils from the Lena Delta, Siberia, *Environ. Microbiol.*, *9*(1), 107–117, doi:10.1111/j.1462-2920.2006.01120.x.
- MacIntyre, S., R. Wanninkhof, and J. P. Chanton (1995), Trace gas exchange across the air-water interface in freshwater and coastal marine environments, in *Biogenic Trace Gases: Measuring Emissions from Soil and Water*, edited by P. Matson and R. Harriss, pp. 52–97, Blackwell, Malden, Mass.
- Moncrieff, J. B., Y. Mahli, and R. Leuning (1996), The propagation of errors in long-term measurements of land-atmosphere fluxes of carbon and water, *Global Change Biol.*, *2*, 231–240, doi:10.1111/j.1365-2486.1996.tb00075.x.
- Moore, C. J. (1986), Frequency response corrections for eddy correlation systems, *Boundary Layer Meteorol.*, *37*, 17–35, doi:10.1007/BF00122754.
- Post, W. M., W. R. Emanuel, P. J. Zinke, and A. G. Stangenberger (1982), Soil carbon pools and world life zones, *Nature*, *298*, 156–159, doi:10.1038/298156a0.
- Rinne, J., T. Riutta, M. Pihlatie, M. Aurela, S. Haapanala, J.-P. Tuovinen, E.-S. Tuittila, and T. Vesala (2007), Annual cycle of methane emission from a boreal fen measured by the eddy covariance technique, *Tellus, Ser. B*, *59*, doi:10.1111/j.1600-0889.2007.00261.x.
- Schuepp, P. H., M. Y. Leclerc, J. I. MacPherson, and R. L. Desjardins (1990), Footprint prediction of scalar fluxes from analytical solutions of the diffusion equation, *Boundary Layer Meteorol.*, *50*, 355–373, doi:10.1007/BF00120530.
- Soil Survey Staff (1998), Keys to soil taxonomy, 8th ed., U.S. Dep. of Agric., Blacksburg, Va.
- Suyker, A. E., S. B. Verma, R. J. Clement, and D. P. Billesbach (1996), Methane flux in a boreal fen: Season-long measurement by eddy correlation, *J. Geophys. Res.*, *101*(D22), 28,637–28,648, doi:10.1029/96JD02751.
- Tokida, T., T. Miyazaki, and M. Mizoguchi (2005), Ebullition of methane from peat with falling atmospheric pressure, *Geophys. Res. Lett.*, *32*, L13823, doi:10.1029/2005GL022949.
- Tokida, T., T. Miyazaki, M. Mizoguchi, O. Nagata, F. Takakai, A. Kagemoto, and R. Hatano (2007), Falling atmospheric pressure as a trigger for methane ebullition from peatland, *Global Biogeochem. Cycles*, *21*, GB2003, doi:10.1029/2006GB002790.
- UNEP/GRID-Arendal (1996), Arctic vegetation zones, *Habitat Conserv. Map 2*, Arendal, Norway, [http://maps.grida.no/go/graphic/arctic\\_vegetation\\_zones](http://maps.grida.no/go/graphic/arctic_vegetation_zones).
- van Huissteden, J., T. C. Maximov, and A. J. Dolman (2005), High methane flux from an arctic floodplain (Indigirka lowlands, eastern Siberia), *J. Geophys. Res.*, *110*, G02002, doi:10.1029/2005JG000010.
- Wagner, D., S. Kobabe, E.-M. Pfeiffer, and H.-W. Hubberten (2003), Microbial controls on methane fluxes from a polygonal tundra of the Lena Delta, Siberia, *Permafrost Periglacial Processes*, *14*(2), 173–185, doi:10.1002/ppp.443.
- Walker, H. J. (1998), Arctic deltas, *J. Coastal Res.*, *14*(3), 718–738.
- Walter, K. M., S. A. Zimov, J. P. Chanton, D. Verbyla, and F. S. Chapin III (2006), Methane bubbling from thaw lakes as a positive feedback to climate warming, *Nature*, *443*, doi:10.1038/nature05040.
- Wesely, M. L., and R. L. Hart (1985), Variability of short term eddy-correlation estimates of mass exchange, in *The Forest-Atmosphere Interaction*, edited by B. A. Hutchison and B. B. Hicks, pp. 591–612, Springer, Dordrecht, Netherlands.
- Whalen, S. C., and W. S. Reeceburgh (1992), Interannual variations in tundra methane emission: A 4-year time series at fixed sites, *Global Biogeochem. Cycles*, *6*(2), 139–159, doi:10.1029/92GB00430.
- Wickland, K. P., R. G. Striegl, J. C. Neff, and T. Sachs (2006), Effects of permafrost melting on CO<sub>2</sub> and CH<sub>4</sub> exchange of a poorly drained black spruce lowland, *J. Geophys. Res.*, *111*, G02011, doi:10.1029/2005JG000099.
- Wille, C., L. Kutzbach, T. Sachs, D. Wagner, and E.-M. Pfeiffer (2008), Methane emission from Siberian arctic polygonal tundra: Eddy covariance measurements and modeling, *Global Change Biol.*, *14*, 1–14, doi:10.1111/j.1365-2486.2008.01586.x.
- Yu, J., W. Sun, J. Liu, J. Wang, J. Yang, and F. X. Meixner (2007), Enhanced net formations of nitrous oxide and methane underneath the frozen soil in Sanjiang wetland, northeastern China, *J. Geophys. Res.*, *112*, D07111, doi:10.1029/2006JD008025.
- Zhang, T., R. G. Barry, K. Knowles, J. A. Heginbottom, and J. Brown (1999), Statistics and characteristics of permafrost and ground-ice distribution in the Northern Hemisphere, *Polar Geogr.*, *23*(2), 132–154.
- Zimov, S. A., E. A. G. Schuur, and F. S. Chapin III (2006a), Permafrost and the Global Carbon Budget, *Science*, *312*(5780), 1612–1613, doi:10.1126/science.1128908.
- Zimov, S. A., S. P. Davydov, G. M. Zimova, A. I. Davydova, E. A. G. Schuur, K. Dutta, and F. S. Chapin III (2006b), Permafrost carbon: Stock and decomposability of a globally significant carbon pool, *Geophys. Res. Lett.*, *33*, L20502, doi:10.1029/2006GL027484.

J. Boike and T. Sachs, Research Unit Potsdam, Alfred Wegener Institute for Polar and Marine Research, Telegrafenberg A43, D-14473 Potsdam, Germany. (torsten.sachs@awi.de)

L. Kutzbach and C. Wille, Institute of Botany and Landscape Ecology, Ernst Moritz Arndt University of Greifswald, Grimmer Strasse 88, D-17487 Greifswald, Germany.